The Relation between the Pressure Gradient in a Liquid Slug and the Radius of the Following Taylor Bubble in Capillary Tubes

Boonchai Lertnuwat
Dept. of Mechanical Engineering, Faculty of Engineering,
Chulalongkorn University, Phayathai Rd., Pathum Wan, Bangkok 10330, Thailand

Abstract

The pressure drop of slug flows in capillary tubes is mostly resulted from the pressure gradient of liquid slugs in the capillary tubes, which can be related to the radius of the Taylor bubbles behind the liquid slugs. The paper proposes a theoretical relation between the pressure gradient in a liquid slug and the radius of the following Taylor bubble in capillary tubes. The present relation is derived by assuming that the flow taking place around a Taylor bubble is incompressible laminar flow. Verification of the present relation is done by comparing the results predicted from the present relation with the results from empirical formulas. The present relation showed not only that it could predict additional pressure gradients, resulted from the presence of the Taylor bubbles. It also agreed well with the empirical results, and also it gave more insights about slug flows, for instance, the critical bubble-to-tube radius ratio and the velocity profiles in liquid slugs.

Keywords: Multiphase flow, Slug flow, Taylor bubble, Falling film and Capillary

1. Nomenclature

1.1 Characters

W	Relative velocity ratio
u	Velocity
Ca	Capillary number ($\mu_l \lvert u_b \rvert / \sigma_{lb}$)
g	Gravity acceleration
j	Superficial velocity
P	Static pressure
l	Length
r	Radius in cylindrical coordinates
t	Time
z	Vertical distance in cylindrical coordinates

1.2 Symbols

α	Volume fraction of gas
β	Ratio of the length of a Taylor bubble to the length of a slug unit .
δ	Percent of relative discrepancy; see (20)
ε	Roughness of tube surface
μ	Viscosity
θ	Angle in cylindrical coordinates
ρ	Density

1.3 Superscripts and Subscripts

b	Bubble
c	Capillary tube
f	Falling film
g	Gas
l	Liquid
lb	Liquid and bubble interface
ls	Liquid slug
r	Radius in cylindrical coordinates
t	Total slug unit
z	Vertical distance in cylindrical coordinates

2. Introduction

Small tubes have been used for many purposes. Catalytic monoliths, which are widely uses in pollution control for vehicle exhausts, are an application of using small tubes. A catalytic monolith consists of a large number of small tubes arranged in a honeycomb shape. A porous washcoat containing the catalyst is covered on the surface of each small tube so that the catalyst reacts with the flow in the small tubes [1]. Another example of using small tubes is hollow fibre ultrafiltration [2] and Smith and

Cui [3]). A module of hollow fibre ultrafiltration consists of a bundle of membrane small tubes ranging from 0.1 to 2.0 mm in diameter. Fluid flows are introduced inside the small tubes. Filtrate passes through the small tube walls and is collected in a shell.

In academic research, the small tubes are sometimes called either microchannels [4,5,6,7] or capillary tubes [8,9,10,11,12]. The diameter of capillary tubes ranges from 1 to 3 mm [11,12] so the flow inside the capillary tubes is usually laminar.

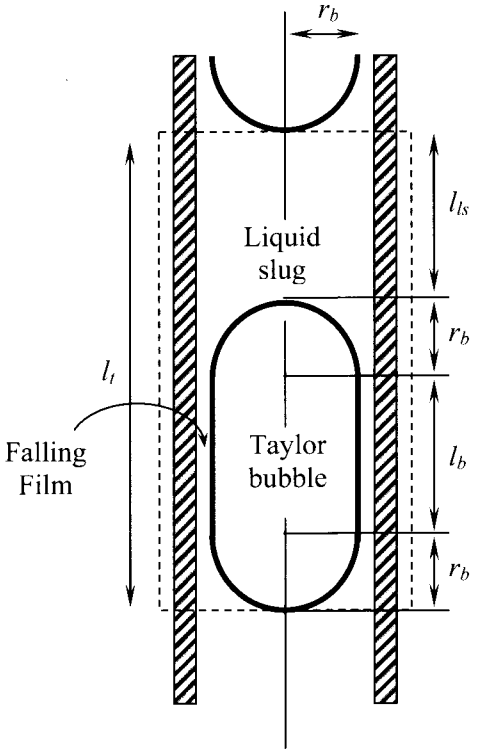

Figure 1: The dimension for a slug unit in a capillary tube.

Many flow patterns can occur in the capillary tubes even though their diameter is small. Slug flows are a regime of flows that often takes place in the capillary tubes. A unit of slug flow is illustrated within the dashed rectangle in Fig. 1. An important parameter of slug flows is the pressure drop across a slug unit. Since the pressure drop across a Taylor bubble is comparatively much smaller than the pressure drop across a liquid slug, it is well known that the pressure drop across a slug unit will be determined if the pressure drop across a liquid slug or pressure gradient in the liquid slug are given. The pressure gradient in liquid slugs depends on the velocity profile, which is affected by the shape of the following Taylor bubble. The objective of this paper is to derive an equation relating the pressure gradient in liquid slugs and the shape (radius) of the following Taylor bubble. The equation will be obtained from the continuity equation and momentum equation with some assumptions, i.e. the flow in liquid slugs is steady, laminar, incompressible and symmetric around tubes centerline.

3. Theoretical Relation

As shown in Fig. 1, a unit of a slug flow in vertical capillary tubes typically is composed of 3 parts, i.e. a liquid slug, Taylor bubble and a falling film. All parts are moving with different velocities. If the Taylor bubble is considered as a reference frame, the velocities of the liquid flow around the Taylor bubble may be depicted as shown in Fig. 2.

Since the diameter of capillary tubes is small, The reynolds number for the liquid flow in the slug is low and the flow is usually laminar. Consequently the velocity profile across the sectional area a-a in the liquid slug (see Fig. 1) can be simply calculated with the Navier-Strokes equations for incompressible flows in cylindrical coordinate as follows.

Continuity equation:

$$\frac{1}{r}\frac{\partial}{\partial r}(ru_r)+\frac{1}{r}\frac{\partial}{\partial \theta}(u_\theta)+\frac{\partial}{\partial z}(u_z)=0 \qquad (1)$$

Momentum equation on z-axis:

$$\rho_l\left(\frac{\partial u_z}{\partial t}+u_r\frac{\partial u_z}{\partial r}+\frac{u_\theta}{r}\frac{\partial u_z}{\partial \theta}+u_z\frac{\partial u_z}{\partial z}\right) = \mu_l\left[\frac{1}{r}\frac{\partial}{\partial r}\left(r\frac{\partial u_z}{\partial r}\right)+\frac{1}{r^2}\frac{\partial^2 u_z}{\partial \theta^2}+\frac{\partial^2 u_z}{\partial z^2}\right] +\rho_l g-\frac{\partial P}{\partial z} \qquad (2)$$

If we consider that the flow in the liquid slug is steady and symmetrical on the z-axis, all terms which are functions of either t or θ will be eliminated from (1) and (2). Furthermore, the flow in the liquid slug will be considered as fully developed along the z direction if the space between the cross sectional area a-a and the

Taylor bubble is greater than one diameter of the capillary tube [10]. Hence, all $\frac{\partial u_z}{\partial z}$ will be eliminated. The equations; (1) and (2), can be reduced as below:

$$\frac{1}{r}\frac{\partial}{\partial r}(ru_r)=0 \qquad (3)$$

$$\rho_l u_r \frac{\partial u_z}{\partial r}=\mu_l \frac{1}{r}\frac{\partial}{\partial r}\left(r\frac{\partial u_z}{\partial r}\right)+\rho_l g-\frac{\partial p}{\partial z} \qquad (4)$$

The reduced continuity equation (3) implies that u_r is zero. Hence, the left-hand-side of (4) is zero, as well.

$$0=\mu_l \frac{1}{r}\frac{\partial}{\partial r}\left(r\frac{\partial u_z}{\partial r}\right)+\rho_l g-\frac{\partial p}{\partial z}$$

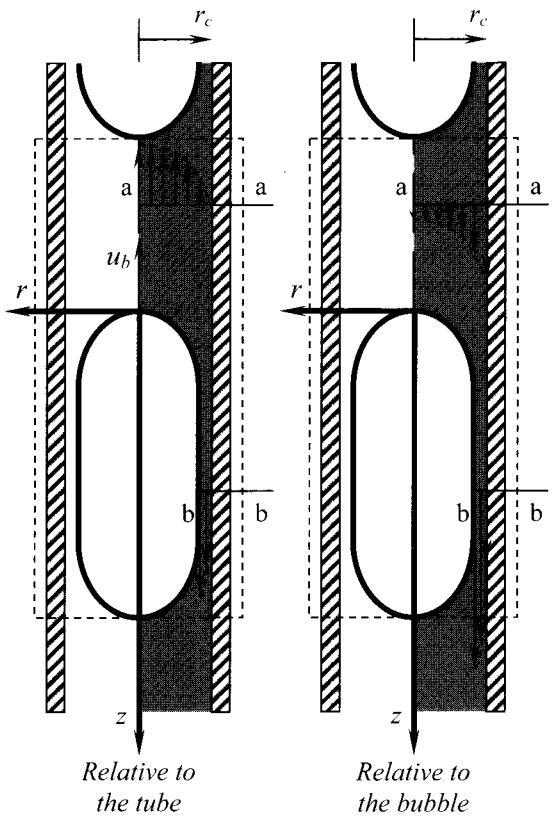

Figure 2: The velocity diagrams of the slug unit in a capillary tube

Integrating for 2 times, we obtain:

$$u_r=\frac{1}{4\mu_l}\left(\frac{\partial P}{\partial z}-\rho_l g\right)r^2+c_1\ln(r)+c_2 \qquad (5)$$

Then, the constants c_1 and c_2 can be determined by applying the following boundary conditions:

1. $\frac{\partial u_r}{\partial r}=0$ when $r=0$
2. $u_r=u_b$ when $r=r_c$

Finally we get the velocity profile across the sectional area (a-a) in the liquid slug as below:

$$u_r=u_b-\frac{1}{4\mu_l}\left(\frac{\partial P}{\partial z}-\rho_l g\right)\left(r_c^2-r^2\right) \qquad (6)$$

The velocity profile across the sectional area b-b in Fig. 2 can be obtained with a similar method. Namely, the set of Navier-Strokes equations; (1) and (2), are integrated under the steady and symmetry conditions. Next, the condition of fully developed flow is applied, in accordance with the assumption that the falling film on the b-b plane is under equilibrium between shear and gravity. This yields:

$$u_r=\frac{1}{4\mu_l}\left(\frac{\partial P}{\partial z}-\rho_l g\right)r^2+c_3\ln(r)+c_4 \qquad (7)$$

which is identical to (5). Mao and Dukler [13] calculated the static pressure in the falling film with:

$$P+\sigma_{lb}K=P_b \qquad (8)$$

where $K=\frac{1}{r_1}+\frac{1}{r_2}$

$$r_1=-\left[1+\left(\frac{\partial r_b}{\partial z}\right)^2\right]\Big/\left(\frac{\partial^2 r_b}{\partial z^2}\right)$$

$$r_2=r_b\sqrt{1+\left(\frac{\partial r_b}{\partial z}\right)^2}$$

Under the equilibrium between shear and gravity, the radius of the Taylor bubble does not change along the z direction, the second term on the left hand side of (8) will be constant. The right hand side of (8) representing the static pressure inside the Taylor bubble is usually assumed to be constant. Therefore the static pressure in the falling film will be constant. The pressure gradient in (7) will be equal to zero. This gives:

$$u_r = -\frac{\rho_l g}{4\mu_l} r^2 + c_3 \ln(r) + c_4 \qquad (9)$$

The constants have to be determined by the following boundary conditions:

1. $\frac{\partial u_r}{\partial r} = 0$ when $r = r_b$
2. $u_r = u_b$ when $r = r_c$

Finally we get the velocity profile across the sectional area (b-b) in the falling film as below:

$$u_r = u_b + \frac{\rho_l g}{4\mu_l}\left[r_c^2 - r^2 + 2r_b^2 \ln\left(\frac{r}{r_c}\right)\right] \qquad (10)$$

Vaporization may occur on a Taylor bubble surface in the case that a temperature change is serious in the flow field, but vaporization is usually low in isothermal flows. According to Fig. 2, the mass flow rates across the sectional areas, a-a and b-b, are equal if the vaporization rate on the Taylor bubble surface is negligibly low. This can be written as:

$$\dot{m}_{slug} = \dot{m}_{film}$$

$$\left(\rho\dot{Q}\right)_{slug} = \left(\rho\dot{Q}\right)_{film}$$

Usually, there are few dispersed bubbles suspended in the flow around the Taylor bubble in the case of flows in capillary tubes, so the flow is assumably an incompressible liquid. Then, the densities are eliminated.

$$\dot{Q}_{ls} = \dot{Q}_f \qquad (11)$$

The flow rate across the sectional area a-a is calculated by integrating the velocity profile equation (6) over the cross sectional area.

$$\dot{Q}_{ls} = \int_0^{r_c} [u_r]\, 2\pi r dr$$

$$= \frac{\pi}{2} r_c^2 \left[2u_b - \frac{1}{4\mu_l}\left(\frac{\partial P}{\partial z} - \rho_l g\right) r_c^2 \right] \qquad (12)$$

Next, the flow rate across the cross sectional area b-b is calculated by integrating the velocity profile equation (10) over the cross sectional area.

$$\dot{Q}_f = \int_{r_b}^{r_c} [u_r]\, 2\pi r dr$$

$$= \frac{\pi}{2} r_c^2 \left\{ 2u_b \left[1 - \left(\frac{r_b}{r_c}\right)^2 \right] + \frac{\rho_l g r_c^2}{4\mu_l}\left[1 - 4\left(\frac{r_b}{r_c}\right)^2 + \left(\frac{r_b}{r_c}\right)^4 \left(3 - 4\ln\left(\frac{r_b}{r_c}\right)\right)\right]\right\} \qquad (13)$$

Substituting (12) and (13) into (11), we obtain the relation between the pressure gradient in a liquid slug and the radius of the following Taylor bubble in capillary tubes as following.

$$\left(\frac{\partial P}{\partial z}\right)_{ls} = \left(\frac{r_b}{r_c}\right)^2 \left\{ \frac{8\mu_l u_b}{r_c^2} + \rho_l g \left[4 - \left(\frac{r_b}{r_c}\right)^2 \left(3 - 4\ln\left(\frac{r_b}{r_c}\right)\right)\right]\right\} \qquad (14)$$

4. Relation Verification

To verify the relation obtained in the previous section, some empirical formulas are employed. The equilibrium radius of Taylor bubbles can be predicted by the Marchessault and Mason's formula, which is referred to in Thulasidas *et al.* [9].

$$\frac{r_c - r_b}{r_c} = -0.05\left(\frac{\mu_l}{\sigma_{lb}}\right)^{\frac{1}{2}} + 0.89\left(\mathrm{Ca}\right)^{\frac{1}{2}},$$

$$\text{for } 7\times10^{-6} < \mathrm{Ca} < 2\times10^{-4} \qquad (15)$$

Next, the pressure gradient on the left hand side of (14) can be estimated by the pressure drop formula used in Garimella *et al.* [5,6].

$$\left(\frac{\partial \hat{P}}{\partial z}\right)_{ls} = f_{ls}\frac{\rho u_{ls}^2}{4r_c}$$

$$\left(\frac{\partial\left(P - \rho_l g z\right)}{\partial z}\right)_{ls} = f_{ls}\frac{\rho u_{ls}^2}{4r_c}$$

$$\left(\frac{\partial P}{\partial z}\right)_{ls} = f_{ls}\frac{\rho u_{ls}^2}{4r_c} + \rho_l g \qquad (16)$$

The friction factor (f) on the right hand side of (16) is calculated by Churchill's equation

[6], which is applicable to both laminar and turbulent flows, and is better than Blasius's turbulent equation [5].

$$f_{ls} = 8\left\{\left(\frac{8}{\mathrm{Re}_{ls}}\right)^{12} + \left[\left[2.457\ln\left(\frac{1}{\left(\frac{7}{\mathrm{Re}_{ls}}\right)^{0.9} + 0.135\frac{\varepsilon}{r_c}}\right)\right]^{16} + \left(\frac{37530}{\mathrm{Re}_{ls}}\right)^{16}\right]^{-1.5}\right\}^{\frac{1}{12}} \quad (17)$$

Herein, Re_{ls} is the Reynolds number of the flow in the liquid slug and is defined as a function of the tube size, the fluid properties and the velocity of the liquid slug.

$$\mathrm{Re}_{ls} = 2\rho_l u_{ls} r_c / \mu_l \quad (18)$$

Thulasidas *et al.* [9] have also suggested the empirical formula proposed by Fairbrother and Stubbs [14] for calculating the relative velocity ratio between Taylor bubbles and liquid slugs as below:

$$W = \frac{u_b - u_{ls}}{u_b} = 1.0(\mathrm{Ca})^{\frac{1}{2}},$$

$$\text{for } 7.5\times10^{-5} < \mathrm{Ca} < 0.014 \quad (19)$$

These can be used to calculate the velocity of the liquid slug and Re_{ls} when Ca (or u_b) is known.

So far, the accuracy of the theoretical relation (14) can be verified at a certain Ca between 7×10^{-6} and 2×10^{-4} by substituting r_b calculated from (15) into (14) to get the theoretical pressure gradient in the case that the fluid properties and r_c are known. Then the empirical pressure gradient will be calculated with (16) – (19) and used as a comparing reference. The results shown in Table 1 – 3 are calculated for the case of air-water slug flows for 3 different radiuses of capillary tube, i.e. 0.5, 1.0 and 1.5mm. The properties of the fluid are (in SI units):

$\rho_l = 998$

$\mu_l = 8.91\times10^{-4}$

$\sigma_{lb} = 7.28\times10^{-2}$

The capillary tubes are considered as smooth pipes, corresponding to laminar conditions, so the roughness of tube surface is set to zero. The percent of relative discrepancy between theoretical and empirical pressure gradients is calculated by:

$$\delta = \frac{(\partial P/\partial z)_{theoretical} - (\partial P/\partial z)_{empirical}}{(\partial P/\partial z)_{empirical}} \times 100\% \quad (20)$$

Table 1: Relative discrepancy between theoretical and empirical pressure gradients at various Ca in the case of 0.5 mm r_c (SI units).

Ca	u_b	r_b	Re_{ls}	δ
7.0×10^{-6}	5.72×10^{-4}	5.016×10^{-4}		
2.0×10^{-5}	1.63×10^{-3}	5.008×10^{-4}		
4.0×10^{-5}	3.27×10^{-3}	5.000×10^{-4}		
6.0×10^{-5}	4.90×10^{-3}	4.993×10^{-4}	5.4	7.07×10^{-3}
8.0×10^{-5}	6.54×10^{-3}	4.988×10^{-4}	7.3	7.64×10^{-3}
1.0×10^{-4}	8.17×10^{-3}	4.983×10^{-4}	9.1	7.59×10^{-3}
1.2×10^{-4}	9.80×10^{-3}	4.979×10^{-4}	10.9	7.00×10^{-3}
1.4×10^{-4}	1.14×10^{-2}	4.975×10^{-4}	12.7	5.93×10^{-3}
1.6×10^{-4}	1.31×10^{-2}	4.971×10^{-4}	14.5	4.42×10^{-3}
1.8×10^{-4}	1.47×10^{-2}	4.968×10^{-4}	16.3	2.49×10^{-3}
2.0×10^{-4}	1.63×10^{-2}	4.965×10^{-4}	18.0	1.95×10^{-4}

Table 2: Relative discrepancy between theoretical and empirical pressure gradients at various Ca in the case of 1.0 mm r_c (SI units).

Ca	u_b	r_b	Re_{ls}	δ
7.0×10^{-6}	5.72×10^{-4}	1.003×10^{-3}		
2.0×10^{-5}	1.63×10^{-3}	1.002×10^{-3}		
4.0×10^{-5}	3.27×10^{-3}	9.999×10^{-4}	7.3	1.46×10^{-3}
6.0×10^{-5}	4.90×10^{-3}	9.986×10^{-4}	10.9	1.79×10^{-3}
8.0×10^{-5}	6.54×10^{-3}	9.976×10^{-4}	14.5	1.93×10^{-3}
1.0×10^{-4}	8.17×10^{-3}	9.966×10^{-4}	18.1	1.92×10^{-3}
1.2×10^{-4}	9.80×10^{-3}	9.958×10^{-4}	21.7	1.76×10^{-3}
1.4×10^{-4}	1.14×10^{-2}	9.950×10^{-4}	25.3	1.47×10^{-3}
1.6×10^{-4}	1.31×10^{-2}	9.943×10^{-4}	28.9	1.06×10^{-3}
1.8×10^{-4}	1.47×10^{-2}	9.936×10^{-4}	32.5	5.39×10^{-4}
2.0×10^{-4}	1.63×10^{-2}	9.929×10^{-4}	36.1	-8.75×10^{-5}

Table 3: Relative discrepancy between theoretical and empirical pressure gradients at various Ca in the case of 1.5 mm r_c (SI units).

Ca	u_b	r_b	Re_{ls}	δ
7.0×10^{-6}	5.72×10^{-4}	1.505×10^{-3}		
2.0×10^{-5}	1.63×10^{-3}	1.502×10^{-3}		
4.0×10^{-5}	3.27×10^{-3}	1.500×10^{-3}		
6.0×10^{-5}	4.90×10^{-3}	1.498×10^{-3}	16.3	7.94×10^{-4}
8.0×10^{-5}	6.54×10^{-3}	1.496×10^{-3}	21.8	8.56×10^{-4}
1.0×10^{-4}	8.17×10^{-3}	1.495×10^{-3}	27.2	8.43×10^{-4}
1.2×10^{-4}	9.80×10^{-3}	1.494×10^{-3}	32.6	7.62×10^{-4}
1.4×10^{-4}	1.14×10^{-2}	1.493×10^{-3}	38.0	6.19×10^{-4}
1.6×10^{-4}	1.31×10^{-2}	1.491×10^{-3}	43.4	4.19×10^{-4}
1.8×10^{-4}	1.47×10^{-2}	1.490×10^{-3}	48.8	1.64×10^{-4}
2.0×10^{-4}	1.63×10^{-2}	1.489×10^{-3}	54.1	-1.42×10^{-4}

According to the tables, the percentages of relative discrepancy between theoretical and empirical pressure gradients are confined within the interval of $\pm10^{-2}$. This confirms the accuracy of the theoretical formula (14). One interesting point is that the discrepancy is high when Ca is low. This may be because u_{ls} is extrapolated from (19) when Ca is lower than the applicable range ($7.5\times10^{-5} < \mathrm{Ca} < 0.014$). Therefore, Re_{ls} calculated from the extrapolated u_{ls}, possibly has some implicit error. However, the discrepancy for the cases of low Ca is still acceptable.

In the tables, some rows with low Ca are omitted since r_b is much greater than r_c. They, thus, are physically meaningless. However δ for low Ca may be obtained by changing the working fluids to adjust the first term on the right hand side of (15).

The corresponding Reynolds numbers in all cases presented in the tables are much less than 2300, which is the conventional criterion for laminar flow in circular pipes.

5. Discussion

The relation (14) shows that the pressure gradient along the tube centerline is a function not only of fluid properties but also of the bubble-to-tube radius ratio. This means that the presence of a Taylor bubble affects the change in the pressure gradient ahead of it. To demonstrate clearly, (14) has to be re-arranged as follows:

$$\left(\frac{\partial P}{\partial z}\right)_{ls} = \frac{8\mu_l u_b}{r_c^2} - \left[1-\left(\frac{r_b}{r_c}\right)^2\right]\frac{8\mu_l u_b}{r_c^2} + \rho_l g\left(\frac{r_b}{r_c}\right)^2\left[4-\left(\frac{r_b}{r_c}\right)^2\left(3-4\ln\left(\frac{r_b}{r_c}\right)\right)\right] \quad (21)$$

The first term on the right hand side of (6.1) is equal to the pressure gradient for the case of one-phase laminar flows in circular pipes, which is calculated by:

$$\left(\frac{\partial P}{\partial z}\right)_l = f_l\frac{\rho_l u_l^2}{4r_c},$$

$$\text{where } f_l = \frac{64}{\mathrm{Re}_l} \text{ and } \mathrm{Re}_l = \frac{2\rho_l u_l r_c}{\mu_l} \quad (22)$$

Since the velocity of one-phase flows is equal to the velocity of liquid slugs, (22) can be re-written in a single formula as:

$$\left(\frac{\partial P}{\partial z}\right)_l = \frac{8\mu_l u_l}{r_c^2} = \frac{8\mu_l u_{ls}}{r_c^2} \quad (23)$$

Next, the velocity of liquid slugs can be determined with (19), that is:

$$u_{ls} = \left[1.0-(\mathrm{Ca})^{\frac{1}{2}}\right]u_b \quad (24)$$

For the case of slug flows in a capillary tube whose Ca is much smaller than unity, the velocity of the liquid slugs can be estimated as:

$$u_{ls} \approx u_b \quad (25)$$

Substituting (25) into (23), we get the pressure gradient for one-phase laminar flow in circular pipes as below:

$$\left(\frac{\partial P}{\partial z}\right)_l \approx \frac{8\mu_l u_b}{r_c^2} \quad (26)$$

Next, subtracting (21) with (26), the difference between the pressure gradient of slug flows and the pressure gradient of one-phase flows is equal to:

$$\left(\frac{\partial P}{\partial z}\right)_{ls,b} = -\left[1-\left(\frac{r_b}{r_c}\right)^2\right]\frac{8\mu_l u_b}{r_c^2} + \rho_l g\left(\frac{r_b}{r_c}\right)^2\left[4-\left(\frac{r_b}{r_c}\right)^2\left(3-4\ln\left(\frac{r_b}{r_c}\right)\right)\right] \quad (27)$$

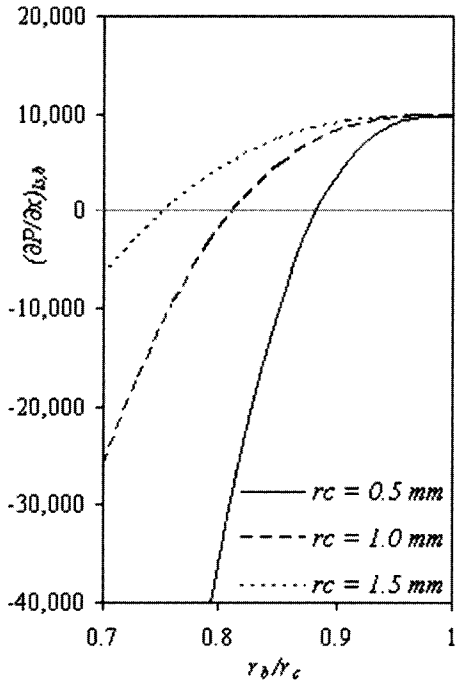

Figure 3: The additional pressure gradients due to the presence of a Taylor bubble in 3 different capillary tubes as a function of bubble-to-tube radius ratio.

Hence, we have found that the presence of a Taylor bubble in capillary tubes added the pressure gradient (27) to the front liquid slug. This is Because u_b is dependent of Ca, which is a function of the bubble-to-tube radius ratio according to (15). The magnitude of the additional pressure gradient of a fluid mixture is a function of bubble-to-tube radius ratio. For example, in the cases of air-water slug flows in capillary tubes, the relations between the additional pressure gradient of the fluid mixture and the bubble-to-tube radius ratio are shown in Fig. 3.

The curves in Fig. 3 reveal that the additional pressure gradient is positive when the bubble-to-tube radius ratio is close to unity. All carves asymptote toward a certain value equal to hydrostatic pressure difference ($\rho_l g$). In contrast, the additional pressure gradient becomes negative when the bubble-to-tube radius ratio is approaches zero. The critical value of the bubble-to-tube radius ratio, where the additional pressure gradient equals to zero depends on the size of capillary tubes. Obviously, Fig. 3 shows that the larger the capillary tube is, the higher the critical bubble-to-tube radius ratio is. It should be noted that the results shown in Fig. 3 are extrapolated to the region of low bubble-to-tube radius ratio where (14) has never been verified. However, the trend of curves gives the idea that there is possibly a critical bubble-to-tube radius ratio for slug flows in capillary tubes.

For slug flows in capillary tubes, some researchers [11,12] assumed that the shape of the Taylor bubble head was a hemispherical cap. The shape of the Taylor bubble head is indeed not exactly a hemispherical cap, but is controlled by either the surface tension of gas-liquid mixtures or Ca [2,8]. However, the relation between the pressure gradient in a liquid slug and the radius of the following Taylor bubble in capillary tubes is independent of the shape of the Taylor bubble head since the shape of the Taylor bubble head is not considered when (14) is derived.

Although (14) is derived for application with vertical slug flows, the application for horizontal slug flows may be possible by little adjustments, namely setting the gravity acceleration (g) to be zero, then, the use of using Figs. 5 and 7 in Thulasidas *et al.* [9] instead of (15) and (19), respectively.

If the dimension of slug flows in capillary tubes can be depicted as shown in Fig. 1, the pressure gradient of the slug unit will be equal to:

$$\left(\frac{\partial P}{\partial x}\right)_t = \left(\frac{\partial P}{\partial x}\right)_{ls}\frac{l_{ls}}{l_t} + \left(\frac{\partial P}{\partial x}\right)_f \frac{l_b + 2r_b}{l_t} \quad (28)$$

Since the pressure gradient occurring in the falling film is very weak, the pressure drop of the slug unit in capillary tubes can be estimated by:

$$\left(\frac{\partial P}{\partial x}\right)_t = \left(\frac{\partial P}{\partial x}\right)_{ls}\frac{l_{ls}}{l_t} \quad 29)$$

According to Thulasidas *et al.* [9], the relationship relating the Taylor bubble velocity with the length of the Taylor bubble and the total length of the slug unit is:

$$\beta = \alpha\left(\frac{r_c}{r_b}\right)^2 + \frac{2r_b}{3l_t} \qquad (30)$$

where $\alpha = \dfrac{j_g}{u_b}$

$$\beta = \frac{l_b + 2r_b}{l_t}$$

Therefore the pressure gradient of a slug unit can be approximately determined in the case that superficial gas velocity (j_g) and the velocity of the Taylor bubble (u_b) are given.

Considering (6), the shape of the velocity profile in liquid slugs is affected by the pressure gradient along the axis of capillary tubes. According to (6), the velocity on the surface of capillary tube ($r = r_c$) is equal to u_b . The velocity will be higher at the centerline of the capillary tube ($r = 0$) if $\partial P/\partial z < \rho_l g$. The parameters which affect the condition that $\partial P/\partial z < \rho_l g$, may be explicitly shown by analyzing the order of magnitude of terms in (14) as follows:

$$O\left[\left(\frac{\partial P}{\partial z}\right)_{ls}\right] = O\left\{\left(\frac{r_b}{r_c}\right)^2\left\{\frac{8\mu_l u_b}{r_c^2} + \rho_l g\left[4 - \left(\frac{r_b}{r_c}\right)^2\left(3 - 4\ln\left(\frac{r_b}{r_c}\right)\right)\right]\right\}\right\} \qquad (31)$$

Since $r_b > 9.9r_c$ for all cases, we approximate that $r_b \approx r_c$. Then (31) yields:

$$O\left[\left(\frac{\partial P}{\partial z}\right)_{ls}\right] \approx O\left\{(1)^2\left\{\frac{8\mu_l u_b}{r_c^2} + \rho_l g\left[4 - (1)^2\left(3 - 4\ln(1)\right)\right]\right\}\right\}$$

$$O\left[\left(\frac{\partial P}{\partial z}\right)_{ls}\right] \approx O\left\{\left(\frac{8\mu_l u_b}{r_c^2} + \rho_l g\right)\right\} \qquad (32)$$

This means that the pressure gradient on the left hand side of (32) will be less than $\rho_l g$ if u_b is negative. According to (24), in the case that Ca is much less than unity, u_b will be negative if u_{ls} is negative (downward flow). Figure 4 illustrates how u_{ls} affects the velocity profile of the air-water slug flows in a capillary tube where r_c = 0.5 mm. For the cases that r_c = 1.0 mm and r_c = 1.5 mm, the velocity profiles are similar to the case that r_c = 0.5 mm. Besides, (32) still informs us that the pressure gradient on the left hand side is more sensitive to the change of u_b in the case that r_c is small.

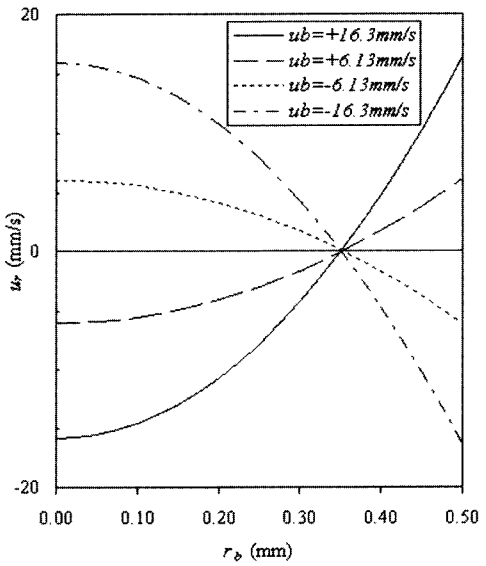

Figure 4: Velocity profiles in liquid slug at various u_{ls} in the case of 0.5-mm r_c .

6. Conclusion

1. The relation between the pressure gradient in a liquid slug and the radius of the following Taylor bubble in capillary tubes (14) has been derived theoretically under some assumptions, i.e.:

1.1 Laminar flow

1.2 Steady flow

1.3 Axis-symmetrical flow

1.4 The liquid slug is much longer than 2D

1.5 The Taylor bubble must be long enough to achieve the equilibrium film thickness

1.6 No dispersed bubble in the liquid slug

1.7 Isothermal conditions

2. The relation (14) is independent of the shape of the Taylor bubble head.

3. Not only for vertical slug flows but the relation (14) may be applied also for horizontal slug flows with some adjustments.

4. Employing (29) and (30), the pressure gradient of slug units can be approximated from the pressure gradient of liquid slugs; (14).

5. The shape of the velocity profile in liquid slugs depends on both u_{ls} and r_c.

6. Furthermore, we can see that the Reynolds number is also a parameter affecting the pressure gradient of slug units by re-arranging the first term in the second parentheses on the right hand side of (14) as follows:

$$\left(\frac{\partial P}{\partial z}\right)_{ls} = \left(\frac{r_b}{r_c}\right)^2 \left\{ \frac{16}{\mathrm{Re}_b} \frac{\rho u_b^2}{r_c} + \rho_l g \left[4 - \left(\frac{r_b}{r_c}\right)^2 \left(3 - 4 \ln\left(\frac{r_b}{r_c}\right)\right)\right]\right\} \quad (33)$$

where $\mathrm{Re}_b = 2\rho_l u_b r_c / \mu_l$

7. References

[1] Woehl, P. and Cerro, R. L., Pressure Drop in Monolith Reactors, Catalysis Today, Vol. 69, pp. 171-174, 2001.

[2] Smith, S., Taha, T. and Cui, Z., Enhancing Hollow Fibre Ultrafiltration Using Slug - Flow a Hydrodynamic Study, Desalination, Vol. 146, pp. 69-74, 2002.

[3] Smith, S. R. and Cui, Z. F., Gas-Slug Enhanced Hollow Fibre Ultrafiltration - An Experimental Study, Journal of Membrane Science, Vol. 242, pp. 117-128, 2004.

[4] Zhao, T. S. and Bi, Q. C., Co-Current Air-Water Two-Phase Flow Patterns in Vertical Triangular Microchannels, International Journal of Multiphase Flow, Vol. 27, pp. 765-782, 2001.

[5] Garimella, S., Killion, J. D. and Coleman, J. W., An Experimentally Validated Model for Two-Phase Pressure Drop in the Intermittent Flow Regime for Circular Microchannels, Journal of Fluids Engineering, Vol. 124, pp. 205-214, 2002.

[6] Garimella, S., Killion, J. D. and Coleman, J. W., An Experimentally Validated Model for Two-Phase Pressure Drop in the Intermittent Flow Regime for Noncircular Microchannels, Journal of Fluids Engineering, Vol. 125, pp. 887-894, 2003.

[7] Garimella, S., Agarwal, A. and Killion, J. D., Condensation Pressure Drop in Circular Microchannels, Heat Transfer Engineering, Vol. 26, pp. 28-35, 2005.

[8] Taha, T. and Cui, Z. F., Hydrodynamics of Slug Flow inside Capillaries, Chemical Engineering Science, Vol. 59, pp. 1181-1190, 2004.

[9] Thulasidas, T. C., Abraham, M. A. and Cerro, R. L., Bubble-Train Flow in Capillaries of Circular and Square Cross Section, Chemical Engineering Science, Vol. 50, pp. 183-199, 1995.

[10] Thulasidas, T. C., Abraham, M. A. and Cerro, R. L., Flow Patterns in Liquid Slugs During Bubble-Train Flow inside Capillaries, Chemical Engineering Science, Vol. 52, pp. 2947-2962, 1997.

[11] Van Baten, J. M. and Krishna, R., CFD Simulation of Mass Transfer from Taylor Bubbles Rising in Circular Capillaries, Chemical Engineering Science, Vol. 59, pp. 2535-2545. 2004.

[12] Van Baten, J. M. and Krishna, R., CFD Simulation of Wall Mass Transfer for Taylor Flow in Circular Capillaries, Chemical Engineering Science, Vol. 60, pp. 1117-1126, 2005.

[13] Mao, Z-S. and Dukler, A. E., The Motion of Taylor Bubbles in Vertical Tubes I. A Numerical Simulation for the Shape and Rise Velocity of Taylor Bubbles in Stagnant and Flowing Liquid, Journal of Computational Physics, Vol. 91, pp. 132-160, 1990.

[14] Fairbrother, F. and Stubbs, A. E., Studies in Electroendosmosis-VI. The Bubble Tube Method of Measurement, Journal of the Chemical Society, Vol. 1, pp. 527-529, 1935